ACCEPTED MANUSCRIPT
Journal of Vacuum Science & Technology A
This is the author's peer reviewed, accepted manuscript. However, the online version of record will be different from this version once it has been copyedited and typeset.
PLEASE CITE THIS ARTICLE AS DOI: 10.1116/6.0002388

Thermal versus radiation-assisted defect annealing in β-Ga_2O_3

Alexander Azarov[1,a], Vishnukanthan Venkatachalapathy[1], In-Hwan Lee[2]

and Andrej Kuznetsov[1]

[1] University of Oslo, Department of Physics, Centre for Materials Science and Nanotechnology, PO Box 1048 Blindern, N-0316 Oslo, Norway

[2] Department of Materials Science and Engineering, Korea University, Seoul 02841, Republic of Korea

Gallium oxide (Ga_2O_3) exhibits complex behavior under ion irradiation since ion-induced disorder affects not only the functional properties, but can provoke polymorphic transformations in Ga_2O_3. Conventional way used to minimize the lattice disorder is by doing post-irradiation anneals. An alternative approach is to prevent the disorder accumulation from the beginning, by doing implants at elevated temperatures, so that significant fraction of the disorder dynamically anneals out in radiation-assisted processes. Here, we use these two approaches for the minimization of radiation disorder in monoclinic β-Ga_2O_3 implanted to a dose below the threshold required for the polymorphic transformations. The results obtained by a combination of channeling and x-ray diffraction techniques revealed that implants at 300 °C effectively suppresses defect formation in β-Ga_2O_3. On the other hand, in order to reach similar crystalline quality in the samples implanted at room temperature, post-irradiation anneals in excess of 900 °C are necessary.

[a] Author to whom correspondence should be addressed: alexander.azarov@smn.uio.no

ACCEPTED MANUSCRIPT
Journal of Vacuum Science & Technology A
This is the author's peer reviewed, accepted manuscript. However, the online version of record will be different from this version once it has been copyedited and typeset.
PLEASE CITE THIS ARTICLE AS DOI: 10.1116/6.0002388

I. INTRODUCTION

Among other wide and ultra-wide bandgap semiconductors, gallium oxide (Ga_2O_3) has recently received tremendous research interest, primarily due to its potential applications for power electronics where energy losses due to switching and transmission are crucial [1,2]. According to theoretical estimations, Ga_2O_3 can provide much better device performance as compared to the current SiC and GaN technologies [3,4]. Furthermore, large diameter highly crystalline Ga_2O_3 wafers can be obtained by conventional growth techniques unlike to SiC and GaN [5].

In the device fabrication technology, ion implantation is one of the prime tools and it can be used for a selective area electronic doping [6], electrical isolation [7] as well as changing magnetic [8] and optical [9] properties of Ga_2O_3 bulk crystals and thin films. However, radiation defects can negatively affect the properties of the material and successful ion beam processing of Ga_2O_3 requires deep understanding of the radiation defect formation mechanisms as well as their thermal evolution. The situation in Ga_2O_3 is also complicated by the polymorphism with different Ga_2O_3 phases exhibiting different crystal structures and, therefore, physical properties [10]. Indeed, it was shown that metastable rhombohedral α-Ga_2O_3 is less susceptible to ion radiation as compared to the most stable monoclinic β-phase [11]. In its turn, β-Ga_2O_3 exhibits phase instability under ion implantation leading to a new phase formation for high enough ion doses [12-15].

One of the most important parameters affecting the defect formation/evolution in the irradiated materials is a temperature [16]. Typically, post-implantation anneals are used to remove radiation defects and activate the implanted impurities [17]. Another approach is related to the variation of the irradiation (sample) temperature that can be very attractive since it affects the defect formation during implantation process [18].

Journal of Vacuum Science & Technology A
ACCEPTED MANUSCRIPT
This is the author's peer reviewed, accepted manuscript. However, the online version of record will be different from this version once it has been copyedited and typeset.
PLEASE CITE THIS ARTICLE AS DOI: 10.1116/6.0002388

The role of the temperature on the radiation defect formation/evolution in Ga_2O_3 is not well studied. Indeed, there are only a few preliminary reports showing that the thermal stability of radiation defects in β-Ga_2O_3 dramatically depends on the implanted dose and ion species [19,20]. In its turn, it was shown that implantation at elevated temperature can be used to partially reduce radiation disorder in heavily Eu implanted β-Ga_2O_3 samples [21]. However, the implantation at elevated temperatures can be used to fully suppress the formation of radiation defects in β-Ga_2O_3 in the low dose regime [22] where accumulated disorder is far below the saturation level [23].

In the present contribution we compare elevated temperature implants with conventional post-implantation thermal treatment as tools to minimize the residual disorder in β-Ga_2O_3 single crystals. We demonstrate that for the implantation doses, below the threshold required to ignite the polymorphic transitions, the dynamic annealing during elevated temperature implants can be beneficial as compared to the post-implantation annealing process.

II. EXPERIMENTAL

In the present work (010) oriented β-Ga_2O_3 single crystals (Tamura Corp.) were implanted with 400 keV $^{58}Ni^+$ ions to a dose of 2×10^{14} cm^{-2}. During the implantation the ion flux was kept constant at 2×10^{12} at/(cm^2s) to avoid dose-rate effects [22]. The implantations were performed maintaining 7° off-angle orientation from normal direction to minimize channeling. The first set of the samples was implanted at different temperatures varied from room temperature (RT) up to 300 °C. The second set of samples were implanted at RT and then subjected to annealing at 200–900 °C for 30 min in air using a conventional tube furnace.

Journal of Vacuum Science & Technology A
ACCEPTED MANUSCRIPT
This is the author's peer reviewed, accepted manuscript. However, the online version of record will be different from this version once it has been copyedited and typeset.
PLEASE CITE THIS ARTICLE AS DOI: 10.1116/6.0002388

After the implantation and/or annealing processes the samples were characterized by a combination of Rutherford backscattering spectrometry in channeling mode (RBS/C) and x-ray diffraction technique. The RBS/C measurements were performed by 1.6 MeV He^+ ions incident along [010] direction and backscattered into a detector placed at 165° relative the incident beam direction. All RBS/C spectra were analyzed using one of the conventional algorithms [24] for extracting the effective number of scattering centres (referred to below as 'relative disorder'). XRD 2theta measurements were performed using the Bruker AXS D8 Discover diffractometer with high-resolution Cu $K_{\alpha 1}$ radiation.

III. RESULTS AND DISCUSSION

A. Dynamic annealing

The role of the irradiation temperature on the disorder formation in the low fluence implanted samples is illustrated by Fig. 1 showing (a) the Ga-parts of RBS/C spectra and corresponding XRD 2theta scans of the samples implanted with Ni ions to 2×10^{14} cm^{-2} at RT, 150 and 300 °C. It is seen from Fig. 1(a) that RT implantation produces a box-like disordered layer extended from the surface until ~200 nm in depth. The damage in this layer is ~90% of the full amorphization level corresponding well to the damage saturation stage typically observed in (010) β-Ga_2O_3 samples [11,23]. Increase of the irradiation temperature dramatically affects the disorder formation and already at 150 °C the damage profile becomes a Gaussian shape with the peak position located deeper as compared to the nuclear energy loss profile with the maximum at R_{pd}=115 nm according to the SRIM code [25] simulations shown by the dash-dotted line in Fig. 1(a). This apparent shift of the 150 °C damage profile can be directly attributed to the enhanced defect annihilation at the sample surface. Further increase of the

Journal of Vacuum Science & Technology A
ACCEPTED MANUSCRIPT
This is the author's peer reviewed, accepted manuscript. However, the online version of record will be different from this version once it has been copyedited and typeset.
PLEASE CITE THIS ARTICLE AS DOI: 10.1116/6.0002388

irradiation temperature up to 300 °C leads to practically no disorder in the implanted region and channeling RBS spectrum becomes close to the virgin one, as clearly seen from Fig. 1(a).

It is important to note that analysis of the XRD 2theta scans of the low fluence samples does not revealed any phase transformations (Fig. 1(b)). Instead, the RT implants results in the formation of shoulder peak at the high-angle side of the (020) reflection centered at 60.9° (see Fig. 1(b)). This shoulder peak is attributed to the compressive strain accumulated in the implanted region [26]. In its turn, a long tail at the right-hand-side of the shoulder peak can be attributed to the large concentration of extended defects [27]. Note that a compressive strain buildup is typical for the implanted (010) β-Ga_2O_3 single crystals [28] that is in contrast to many other semiconductor materials exhibiting tensile strain accumulation under ion irradiation [29]. For 150 °C implantation the value of the strain becomes lower as compared to that of RT sample, however, a broadness of the (020) reflection peak becomes larger. Finally, for 300 °C implantation the XRD 2theta scan resembles the virgin one indicating nearly perfect crystalline structure.

B. Thermal annealing

The defect annealing kinetics in the course of the post-implantation thermal treatment is illustrated by Fig. 2 showing (a) RBS/C spectra and (b) corresponding XRD 2theta scans of the RT implanted sample before and after different anneals. It can be seen from Fig. 2(a) that defect annealing exhibits distinct two stage annealing behavior. Indeed, the first stage occurring at relatively low temperatures and already after 300-400 °C anneals the thickness of the disordered layer decreases starting from the inner boundary. This effect is accompanied by a strain relaxation as can be seen from the XRD results (Fig. 2(b)). Increase of the annealing temperature up to 500 °C leads to the

Journal of Vacuum Science & Technology A
ACCEPTED MANUSCRIPT
This is the author's peer reviewed, accepted manuscript. However, the online version of record will be different from this version once it has been copyedited and typeset.
PLEASE CITE THIS ARTICLE AS DOI: 10.1116/6.0002388

efficient disorder removal at the sample surface (Fig. 2(a)) and, according to the XRD results (Fig. 2(b)), the tail at the right-hand-side of the (020) reflection vanishes indicating an improvement of the crystal quality.

Note that according to the RBS/C results, the maximum disorder in the implanted region remains practically unchanged for the temperatures up to 500 °C. However, the disorder exhibits gradual annealing for the temperatures ≥600 °C and its maximal amplitude decreases indicating the second annealing stage. The RBS/C results also show that despite an efficient defect annealing at this stage the channeling spectra are still far from the virgin one even after the highest annealing temperature used (900 °C). Furthermore, the 900 °C RBS/C spectrum is characterized by a high dechanneling yield that may indicate formation of the extended defects such as stacking faults and dislocation loops [30]. So, the temperature in excess of 900 °C is required to complete restore the crystal lattice after implantation. Interestingly enough that XRD 2theta scans of the 500 and 700 °C annealed samples demonstrates small shoulder on the left-hand-side of the (020) reflection (Fig. 2(b)). This shoulder can be attributed to the tensile strain formation due to defect transformation, for example, the growth of the extended defects.

C. Discussion

The results shown in Figs. 1 and 2 are summarized in Fig. 3 where the relative disorder in the maximum of its distribution is plotted as a function of the irradiation/annealing temperature. It is clearly seen that the difference between the two approaches is spectacular and the “hot” implantation provides better results in terms of defect minimization as compared to the post-implantation annealing. The obtained results can be understood in terms of the different processes involved in these two regimes. Indeed, irradiation temperature mainly affects dynamic annealing processes,

Journal of Vacuum Science & Technology A
ACCEPTED MANUSCRIPT
This is the author's peer reviewed, accepted manuscript. However, the online version of record will be different from this version once it has been copyedited and typeset.
PLEASE CITE THIS ARTICLE AS DOI: 10.1116/6.0002388

such as defect annihilation, occurring during implantation. The residual number of defects in the irradiated target is determined by the balance between defect generation and defect annihilation rates. Efficiency of the latter process increases with increasing irradiation temperature, so that the defect formation is suppressed at high temperatures. It should be noted that a defect generation rate can be also affected by an ion flux and its changing can lead to the shift of the temperature range where the defect formation strongly depends on the irradiation temperature [22]. However, in our study all the implants were performed at a constant ion flux, as mentioned above.

In contrast, the post-implantation annealing affects mainly the thermal stability of the defects formed during implantation. It should be noted that exact identification of the defects based n the RBS/C and XRD results alone is challenging. However, previous results indicated that for low dose regime the disorder region contains mainly uncorrelated defect structures such as point defects and defect clusters [14]. For higher doses corresponding to the saturation stage of the disorder accumulation (~90% of the full amorphization level) formation of more complex defects can be anticipated [20]. It should be pointed out that no indication of phase transitions were found in the implanted samples, so the different annealing stages can be attributed to the different thermal stability of the defects formed during implantation.

It should be noted that both the disorder formation as well as the temperature range required to suppress or anneal out the ion-induced disorder in β-Ga_2O_3 are different from those of its major rival GaN. Indeed, it was demonstrated that GaN is more radiation resistant as compared to β-Ga_2O_3 [11]. The disorder in GaN forms two distinct peaks located at the surface and in the crystal bulk which have a different microstructure as well as thermal stability [31]. Moreover, it was shown that increasing irradiation temperature up to 550 °C is not enough to efficiently suppress disorder

Journal of Vacuum Science & Technology A
ACCEPTED MANUSCRIPT
This is the author's peer reviewed, accepted manuscript. However, the online version of record will be different from this version once it has been copyedited and typeset.
PLEASE CITE THIS ARTICLE AS DOI: 10.1116/6.0002388

formation [32]. In its turn, the temperatures in excess of 1150 °C are needed to anneal out the ion-induced disorder in the GaN bulk [33].

IV. CONCLUSIONS

The roles of the irradiation temperature and post-implantation annealing on defect formation in (010) oriented β-Ga_2O_3 single crystals were compared for the implanted doses below the threshold for the phase transitions. We demonstrated that the elevated temperature implants can be used to efficiently suppress radiation defect formation, so that significant reduction of the disorder is observed already at 300 °C. In its turn, defect removal in the course of the conventional post-implantation anneals occurs via two stages and the temperatures in excess of 900 °C required to restore the crystal lattice.

ACKNOWLEDGMENTS

M-ERA.NET Program is acknowledged for financial support via GOFIB project (administrated by the Research Council of Norway project number 337627). The international collaboration was enabled through the INTPART and UTFORSK Programs at the Research Council of Norway and the Directorate for Higher Education and Skills in Norway (NEARTEMS project number 322382 and SPECTRINKO project number UTF-2021/10210). The Research Council of Norway is also acknowledged for the support to the Norwegian Micro- and Nano-Fabrication Facility, NorFab, project number 295864.

ACCEPTED MANUSCRIPT
Journal of Vacuum Science & Technology A

This is the author's peer reviewed, accepted manuscript. However, the online version of record will be different from this version once it has been copyedited and typeset.
PLEASE CITE THIS ARTICLE AS DOI: 10.1116/6.0002388

AUTHOR DECLARATIONS

Conflict of interest

The authors have no conflicts to disclose.

DATA AVAILABILITY

The data that supports the findings of this study are available within the article.

Journal of Vacuum Science & Technology A
ACCEPTED MANUSCRIPT
This is the author's peer reviewed, accepted manuscript. However, the online version of record will be different from this version once it has been copyedited and typeset.
PLEASE CITE THIS ARTICLE AS DOI: 10.1116/6.0002388

1. S. J. Pearton, J. Yang, P. H. Cary, F. Ren, J. Kim, M. J. Tadjer, and M. A. Mastro, "A review of Ga_2O_3 materials, processing, and devices", Appl. Phys. Rev. **5**, 011301 (2018).
2. M. Higashiwaki, A. Kuramata, H.Murakami, and Y. Kumagai, "State-of-the-art technologies of gallium oxide power devices", J. Phys. D: Appl. Phys. **50**, 333002 (2017).
3. M. Higashiwaki, K. Sasaki, A. Kuramata, T. Masui, and S. Yamakoshi, "Gallium oxide (Ga_2O_3) metal-semiconductor field-effect transistors on single-crystal β-Ga_2O_3 (010) substrates", Appl. Phys. Lett. **100**, 013504 (2012).
4. M. J. Tadjer, "Toward gallium oxide power electronics", Science **378**, 724 (2022).
5. Z. Galazka, "β-Ga_2O_3 for wide-bandgap electronics and optoelectronics", Semicond. Sci. Tech. **33**, 113001 (2018).
6. M. H. Wong, K. Goto, H. Murakami, Y. Kumagai, and M Higashiwaki, "Current aperture vertical β-Ga_2O_3 MOSFETs fabricated by N- and Si-ion implantation doping", IEEE Electr. Device L. **40**, 431 (2019).
7. K. Tetzner, A. Thies, B. T. Eldad, F. Brunner, Günter Wagner, and J. Würfl, "Selective area isolation of β-Ga_2O_3 using multiple energy nitrogen ion implantation", Appl. Phys. Lett. **113**, 172104 (2018).
8. B. Peng, Y. Zhang, Y. Wang, L. Yuan, L. Dong, and R. Jia, "Observation of room temperature ferromagnetism and exchange bias in a $^{55}Mn^+$ ion-implanted unintentionally doped β-Ga_2O_3 single crystal", J. Magn. Magn. Mater. **506**, 166687 (2020).
9. M. Peres, E. Nogales, B. Mendez, K. Lorenz, M. R. Correia, T. Monteiro, and N. Ben Sedrine, "Eu activation in β-Ga_2O_3 MOVPE thin films by ion implantation", ECS J. Solid State Sc. **8**, Q3097 (2019).

Journal of Vacuum Science & Technology A
ACCEPTED MANUSCRIPT
This is the author's peer reviewed, accepted manuscript. However, the online version of record will be different from this version once it has been copyedited and typeset.
PLEASE CITE THIS ARTICLE AS DOI: 10.1116/6.0002388

10. K. Kaneko, K. Uno, R. Jinno, and S. Fujita, "Prospects for phase engineering of semi-stable Ga_2O_3 semiconductor thin films using mist chemical vapor deposition", J. Appl. Phys. **131**, 090902 (2022).

11. A. I. Titov, K. V. Karabeshkin, A. I. Struchkov, V. I. Nikolaev, A. Azarov, D. S. Gogova, and P. A. Karaseov, "Comparative study of radiation tolerance of GaN and Ga_2O_3 polymorphs", Vacuum **200**, 111005 (2022).

12. E. A. Anber, D. Foley, A. C. Lang, J. Nathaniel, J. L. Hart, M. J. Tadjer, K. D. Hobart, S. Pearton, and M. L. Taheri, "Structural transition and recovery of Ge implanted β-Ga_2O_3", Appl. Phys. Lett. **117**, 152101 (2020).

13. T. Yoo, X. Xia, F. Ren, A. Jacobs, M. J. Tadjer, S. Pearton, and H. Kim, "Atomic-scale characterization of structural damage and recovery in Sn ion-implanted β-Ga_2O_3", Appl. Phys. Lett. **121**, 072111 (2022).

14. A. Azarov, C. Bazioti, V. Venkatachalapathy, P. Vajeeston, E. Monakhov, and A. Kuznetsov, "Disorder-induced ordering in gallium oxide polymorphs", Phys. Rev. Lett. **128**, 015704 (2022).

15. J. García-Fernández, S. B. Kjeldby, P. D. Nguyen, O. B. Karlsen, L. Vines, and Ш. Prytz, " Formation of γ-Ga_2O_3 by ion implantation: Polymorphic phase transformation of β-Ga_2O_3" Appl. Phys. Lett. **121**, 191601 (2022).

16. E. Wendler, "Mechanisms of damage formation in semiconductors", Nucl. Instrum. Meth. B **267**, 2680 (2009).

17. V. Heera, D. Panknin, and W. Skorupa, "p-Type doping of SiC by high dose Al implantation -problems and progress", Appl. Surf. Sci. **184**, 307 (2001).

18. J. B. Wallace, L. B. Bayu Aji, L. Shao, and S. O. Kucheyev, "Dynamic annealing in Ge studied by pulsed ion beams", Sci. Rep. **7**, 13182 (2017).

19. S. B. Kjeldby, A. Azarov, P. D. Nguyen, V. Venkatachalapathy, R. Mikšová, A. Macková, A. Kuznetsov, Ø. Prytz, and L. Vines, "Radiation-induced defect

ACCEPTED MANUSCRIPT
Journal of Vacuum Science & Technology A
This is the author's peer reviewed, accepted manuscript. However, the online version of record will be different from this version once it has been copyedited and typeset.
PLEASE CITE THIS ARTICLE AS DOI: 10.1116/6.0002388

accumulation and annealing in Si-implanted gallium oxide", J. Appl. Phys. **131**, 125701 (2022).

20. M. J. Tadjer, C. Fares, N. A. Mahadik, J. A. Freitas Jr., D. Smith, R. Sharma, M. E. Law, F. Ren, S. J. Pearton, and A. Kuramata, "Damage recovery and dopant diffusion in Si and Sn ion implanted β-Ga_2O_3", ECS J. Solid State Sc. **8**, Q3133 (2019).

21. M. Peres, K. Lorenz, E. Alves, E. Nogales, B. Méndez, X. Biquard, B. Daudin, E. G. Víllora, and K. Shimamura, "Doping β-Ga_2O_3 with europium: influence of the implantation and annealing temperature", J. Phys. D: Appl. Phys. **50**, 325101 (2017).

22. A. Azarov, V. Venkatachalapathy, E. V. Monakhov, and A. Yu. Kuznetsov, "Dominating migration barrier for intrinsic defects in gallium oxide: dose-rate effect measurements", Appl. Phys. Lett. **118**, 232101 (2021).

23. E. Wendler, E. Treiber, J. Baldauf, S. Wolf, and C. Ronning, "High-level damage saturation below amorphisation in ion implanted β-Ga_2O_3", Nucl. Instrum. Meth. B **379**, 85 (2016).

24. K. Schmid, "Some new aspects for the evaluation of disorder profiles in silicon by backscattering", Radiat. Eff. **17**, 201 (1973).

25. J. F. Ziegler, M. D. Ziegler, and J. P. Biersack, "SRIM—the stopping and range of ions in matter (2010)", Nucl. Instrum. Meth. B **268,** 1818 (2010).

26. A. Debelle and A. Declémy, "XRD investigation of the strain/stress state of ion-irradiated crystals", Nucl. Instrum. Meth. B **268**, 1460 (2010).

27. M. A. Moram and M. E. Vickers, "X-ray diffraction of III-nitrides", Rep. Prog. Phys. **72**, 036502 (2009).

Journal of Vacuum Science & Technology A
ACCEPTED MANUSCRIPT
This is the author's peer reviewed, accepted manuscript. However, the online version of record will be different from this version once it has been copyedited and typeset.
PLEASE CITE THIS ARTICLE AS DOI: 10.1116/6.0002388

28. A. Azarov, V. Venkatachalapathy, P. Karaseov, A. Titov, K. Karabeshkin, A. Struchkov, and A. Kuznetsov, “Interplay of the disorder and strain in gallium oxide”, Sci. Rep. **12**, 15366 (2022).

29. D. R. Pereira, C. Díaz-Guerra, M. Peres, S. Magalhães, J. G. Correia, J. G. Marques, A. G. Silva, E. Alves, and K. Lorenz, “Engineering strain and conductivity of MoO_3 by ion implantation”, Acta Mater. **169**, 15 (2019).

30. A. Turos, P. Jozwik, L. Nowicki, and N. Sathish, “Ion channeling study of defects in compound crystals using Monte Carlo simulations”, Nucl. Instrum. Meth. B **332**, 50 (2014).

31. I.-T. Bae, W. Jiang, C. Wang, W. J. Weber, and Y. Zhang, “Thermal evolution of microstructure in ion-irradiated GaN”, J. Appl. Phys. **105**, 083514 (2009)

32. S. O. Kucheyev, J. S. Williams, J. Zou, C. Jagadish, and G. Li, “The effects of ion mass, energy, dose, flux and irradiation temperature on implantation disorder in GaN”, Nucl. Instrum. Meth. B **178**, 209 (2001).

33. C. Liu, A. Wenzel, J. W. Gerlach, X. F. Fan, and B. Rauschenbach, “Annealing study of ion implanted GaN”, Surf. Coat. Techn. **128-129**, 455 (2000).

Journal of Vacuum Science & Technology A
ACCEPTED MANUSCRIPT
This is the author's peer reviewed, accepted manuscript. However, the online version of record will be different from this version once it has been copyedited and typeset.
PLEASE CITE THIS ARTICLE AS DOI: 10.1116/6.0002388

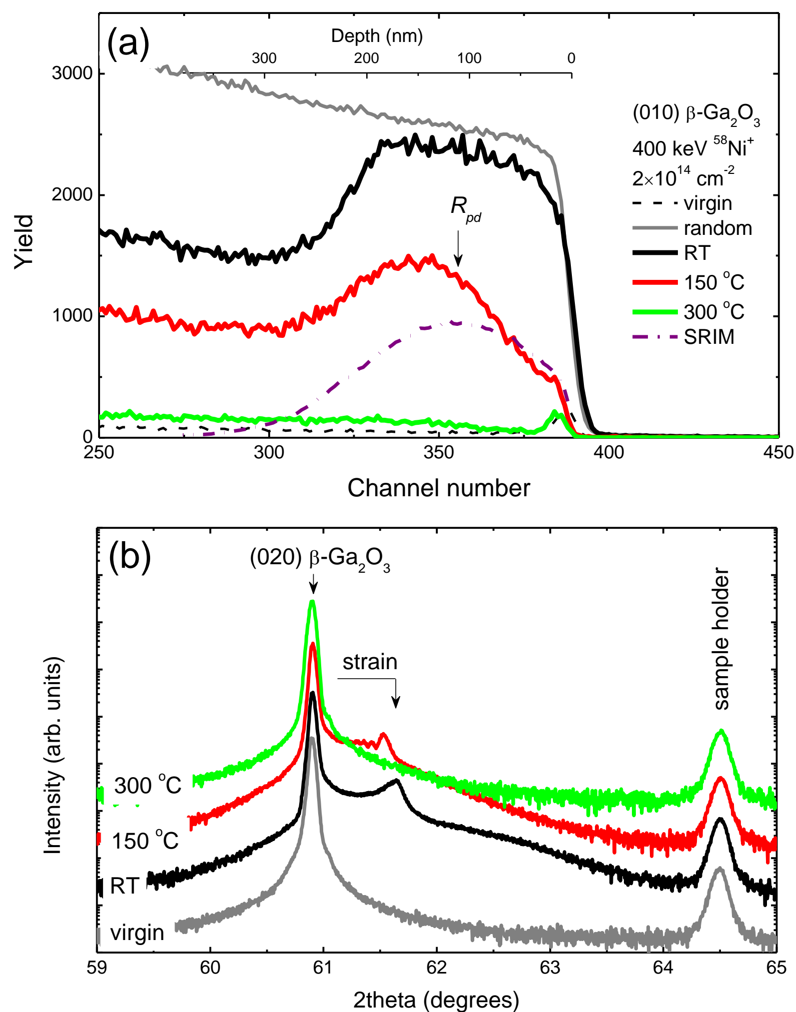

FIG. 1 (a) RBS/C spectra and (b) corresponding XRD 2theta scans across of (010) β-Ga_2O_3 implanted with 400 keV Ni ions to 2×10^{14} cm^{-2} at different temperatures as indicated in the legends. The virgin (unimplanted) spectra/scans are shown in corresponding panels for comparison. The nuclear energy loss profile calculated with the SRIM code simulations is also shown in panel (a) by the dash-dotted line in correlation with the Ga depth scale. The peak at 64.5° in panel (b) corresponds to the sample holder.

Journal of Vacuum Science & Technology A
ACCEPTED MANUSCRIPT
This is the author's peer reviewed, accepted manuscript. However, the online version of record will be different from this version once it has been copyedited and typeset.
PLEASE CITE THIS ARTICLE AS DOI: 10.1116/6.0002388

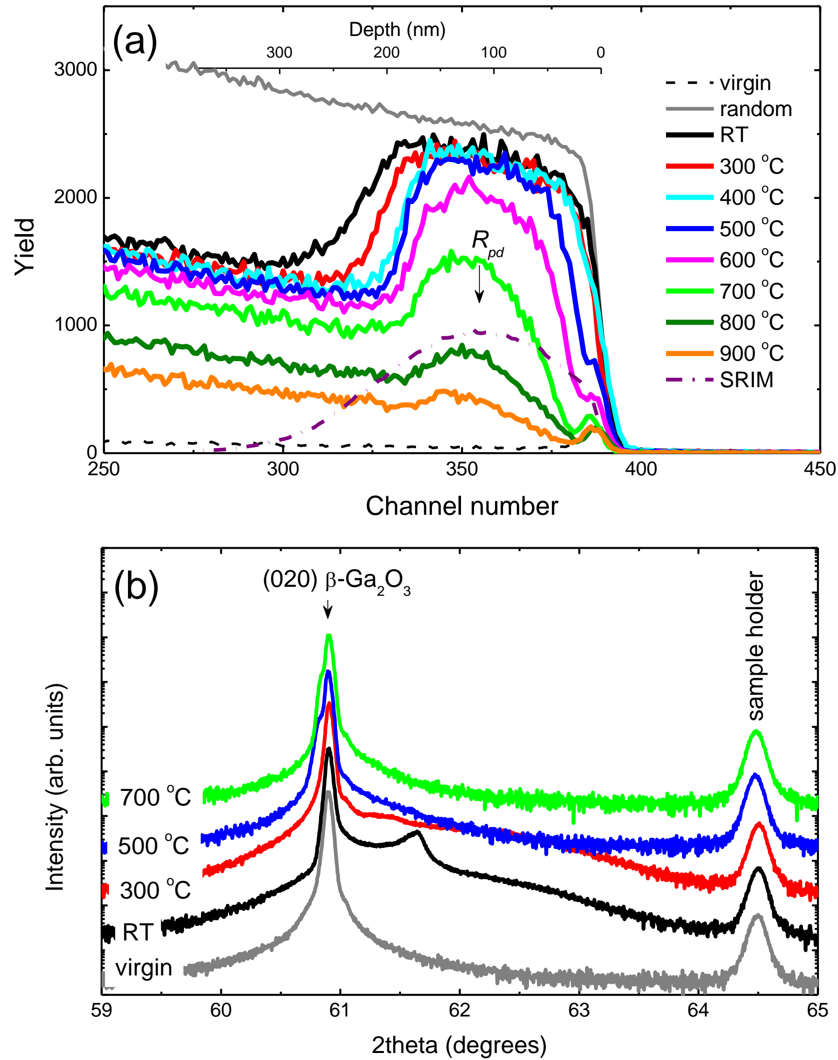

FIG. 2 (a) Ga-parts of the RBS/C spectra and (b) corresponding XRD 2theta scans of (010) β-Ga_2O_3 sample implanted with 400 keV Ni ions to 2×10^{14} cm^{-2} before and after annealing at different temperatures as indicated in the legends. The virgin (unimplanted) spectra/scans are shown in corresponding panels for comparison. The nuclear energy loss profile calculated with the SRIM code simulations is also shown in panel (a) by the dash-dotted line in correlation with the Ga depth scale. The peak at 64.5° in panel (b) corresponds to the sample holder.

ACCEPTED MANUSCRIPT
Journal of Vacuum Science & Technology A
This is the author's peer reviewed, accepted manuscript. However, the online version of record will be different from this version once it has been copyedited and typeset.
PLEASE CITE THIS ARTICLE AS DOI: 10.1116/6.0002388

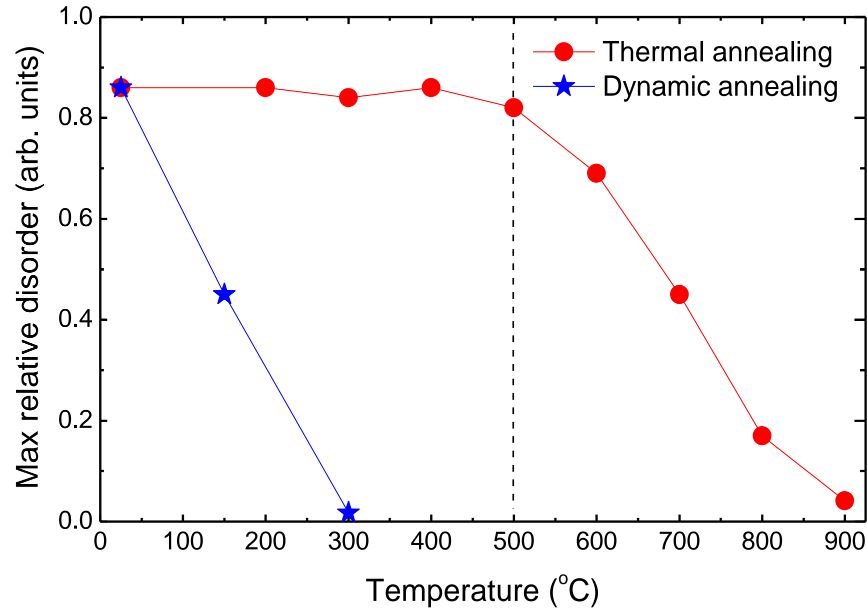

FIG. 3 Maximum relative disorder, as deduced from the RBS/C spectra, in (010) β-Ga_2O_3 samples implanted with 400 keV Ni ions to 2×10^{14} cm^{-2} as a function of implantation/annealing temperature.

Journal of Vacuum Science & Technology A
ACCEPTED MANUSCRIPT
This is the author's peer reviewed, accepted manuscript. However, the online version of record will be different from this version once it has been copyedited and typeset.
PLEASE CITE THIS ARTICLE AS DOI: 10.1116/6.0002388

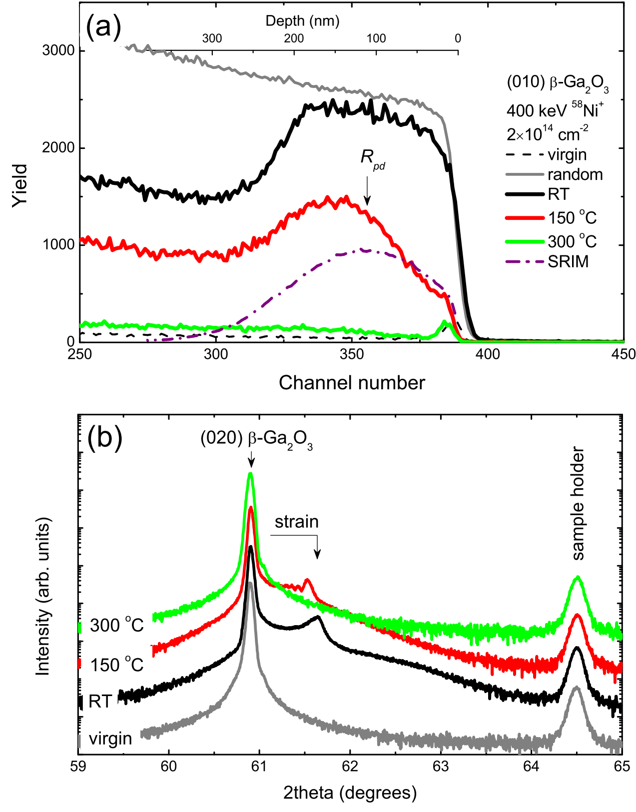

Journal of Vacuum Science & Technology A

ACCEPTED MANUSCRIPT

This is the author's peer reviewed, accepted manuscript. However, the online version of record will be different from this version once it has been copyedited and typeset.

PLEASE CITE THIS ARTICLE AS DOI: 10.1116/6.0002388

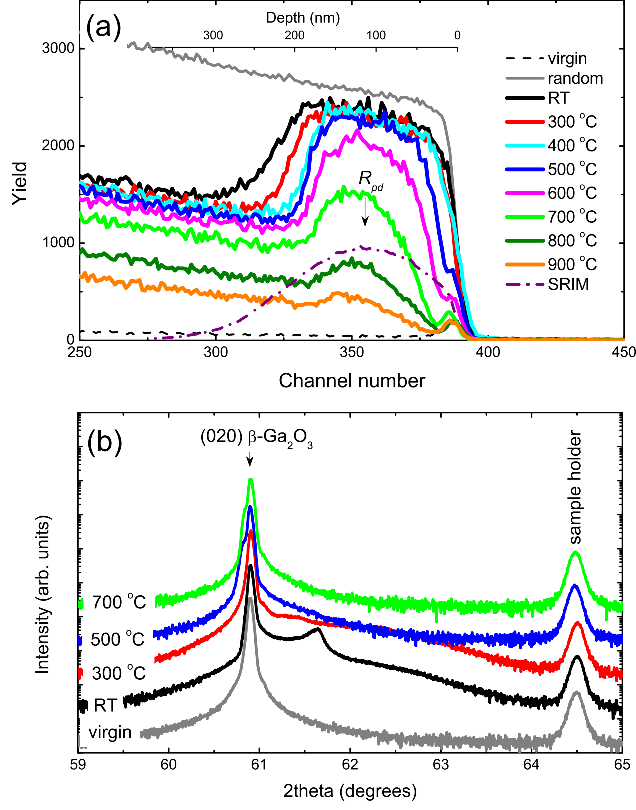

Journal of Vacuum Science & Technology A
ACCEPTED MANUSCRIPT
This is the author's peer reviewed, accepted manuscript. However, the online version of record will be different from this version once it has been copyedited and typeset.
PLEASE CITE THIS ARTICLE AS DOI: 10.1116/6.0002388